International Journal of Pharmaceutics 653 (2024) 123904

Contents lists available at ScienceDirect

International Journal of Pharmaceutics

journal homepage: www.elsevier.com/locate/ijpharm

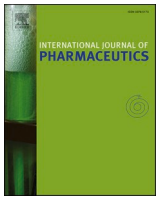

Modulating the release of bioactive molecules of human mesenchymal stromal cell secretome: Heparinization of hyaluronic acid-based hydrogels

Fabio Salvatore Palumbo [a], Calogero Fiorica [a], Anna Paola Carreca [b], Gioacchin Iannolo [c], Giovanna Pitarresi [a], Giandomenico Amico [b], Gaetano Giammona [a], Pier Giulio Conaldi [c], Cinzia Maria Chinnici [d,*]

[a] Dipartimento di Scienze e Tecnologie Biologiche Chimiche e Farmaceutiche (STEBICEF), Università degli Studi di Palermo, Via Archirafi 32, 90123 Palermo, Italy
[b] Regenerative Medicine and Immunotherapy Unit, Fondazione Ri.MED c/o IRCCS ISMETT, via E. Tricomi 5, 90127 Palermo, Italy
[c] Department of Research, IRCCS ISMETT, via E. Tricomi 5, 90127 Palermo, Italy
[d] Cell Therapy Group, Fondazione R.MED c/o IRCCS ISMETT, via E. Tricomi 5, 90127 Palermo, Italy

ARTICLE INFO

Keywords:
Mesenchymal stromal cells
Hyaluronic acid hydrogel
Heparin
Secretome delivery

ABSTRACT

An amine derivative of hyaluronic acid (HA) was crosslinked to obtain a 3D dried sponge. The sponge was subsequently rehydrated using secretome from human mesenchymal stromal cells (MSCs), resulting in the formation of a hydrogel. The release kinetics analysis demonstrated that the hydrogel effectively sustained secretome release, with 70% of the initially loaded wound-healing-associated cytokines being released over a 12-day period. Tuning the hydrogel properties through heparin crosslinking resulted in a biomaterial with a distinct mechanism of action. Specifically, the presence of heparin enhanced water uptake capacity of the hydrogel and increased its sensitivity to enzymatic degradation. Notably, the heparin crosslinking also led to a significant retention of cytokines within the hydrogel matrix. Overall, the secretome-rehydrated HA hydrogel holds promise as a versatile device for regenerative medicine applications: the non-heparinized hydrogel may function as a biomaterial with low reabsorption rates, sustaining the release of bioactive molecules contained in MSC secretome. In contrast, the heparinized hydrogel may serve as a depot of bioactive molecules with faster reabsorption rates. Given its patch-like characteristic, the HA-based hydrogel appears suitable as topical treatment for external organs, such as the skin.

1. Introduction

Growing evidence indicates that mesenchymal stromal cells (MSCs) function as a reservoir of bioactive factors responsible for their therapeutic effects, collectively known as secretome (Caplan, 2017; Vizoso et al., 2017). MSC secretome has demonstrated the ability to replicate the therapeutic benefits observed when using cells in various animal models of diseases (Vizoso et al., 2017), to the point of being considered a valid alternative to cell transplantation. Consequently, secretome-based therapy is emerging as a cell-free option to conventional cell therapy for the restoration of organ functions. This approach is currently under investigation in preclinical and clinical trials. However, despite substantial evidence from preclinical animal models, there is still a limited number of clinical trials assessing the safety and efficacy of MSC secretome (Giovannelli et al., 2023). The advantages of using secretome-based therapy versus cell therapy include a greater safety profile and the opportunity to be manufactured in advance in large quantities in an off-the-shelf fashion (Tran & Damaser, 2015; Vizoso et al., 2017). Nevertheless, critical aspects of the approach encompass pharmacokinetics and half-life of secretome bioactive components (Drago et al., 2013; Gwam et al., 2021). Indeed, the administration of soluble agents requires the presence of delivery devices that protect these agents from undesired degradation and sustain their release to ensure an effective exposure time to the target organ (Censi et al., 2012; Liechty & Peppas, 2012). Delivery devices are based on natural or synthetic polymers. In both cases, the hydrogel formulation has been widely investigated in various biomedical fields, including drug delivery (Jiao et al., 2016), tissue engineering, and regenerative medicine applications, such as wound healing (Huang et al., 2017; Liang et al., 2021), cartilage repair (Palumbo et al., 2012a; Palumbo, Fiorica, Di Stefano, et al., 2015a), and

* Corresponding author at: Regenerative Medicine and Immunotherapy Unit, Fondazione Ri.MED, Via E. Tricomi, 5, 90127 Palermo, Italy.
E-mail address: cchinnici@fondazionerimed.com (C. Maria Chinnici).

https://doi.org/10.1016/j.ijpharm.2024.123904
Received 21 November 2023; Received in revised form 9 February 2024; Accepted 10 February 2024
Available online 12 February 2024

cardiovascular diseases (Liao et al., 2020). Hydrogels are 3D networks of hydrophilic polymers crosslinked chemically or physically, with robust water retention capabilities (Chai et al., 2017). Their crosslinking status can be further modified to tune their properties, such as swelling ability or the hydrolytic and enzymatic degradation profile (Freudenberg et al., 2015; Tsurkan et al., 2013). Due to biocompatibility concerns, natural polymer-based hydrogels are preferred over synthetic polymer hydrogels. In this context, hyaluronic acid (HA), a major constituent of vertebrate extracellular matrix (ECM), stands out as a versatile biomaterial extensively investigated in a wide range of biomedical applications (Miller et al., 2014). HA offers numerous sites for different crosslinking strategies. Consequently, it can be tailored for the desired applications. For instance, HA crosslinking has been used to reduce the rapid *in vivo* enzymatic degradation of the biomaterial or to achieve prolonged drug delivery (Xu et al., 2012).

In previous studies, we have described a procedure for functionalizing HA with ethylenediamine (EDA) groups resulting in the derivative HA-EDA, and discussed its potential for cartilage regeneration applications (Palumbo et al., 2012b). Further crosslinking of HA-EDA enabled the production of a 3D porous hydrogel (HA-EDA/HA), which was subjected to freeze-drying and stored in the form of sponges. These sponges readily turned into a hydrogel upon rehydration with aqueous solutions (Palumbo et al., 2015b).

Here, our aim is to develop a HA-based hydrogel rehydrated with secretome for future applications of regenerative medicine, particularly for skin wound healing. Freeze-dried sponges were integrated with secretome collected from cultured human fetal dermal MSCs (Chinnici et al., 2014, 2020; Gaetani et al., 2018). Additionally, we synthesized a heparin-crosslinked hydrogel designed to exhibit enhanced affinity for secretome bioactive molecules. Both heparin-free and heparin-crosslinked hydrogels underwent physicochemical characterization. Moreover, their ability to sustain secretome release was assessed through Luminex-based quantification, focusing on a panel of growth factors and chemokines known for their key role in angiogenesis and wound healing (Gillitzer & Goebeler, 2001). Finally, the biological activity of the released secretome was evaluated using *in vitro* cell-based assays of angiogenesis and cell migration.

2. Materials and methods

HA (2000 kDa) was purchased from Altergon Italia Srl (Italy). HA with a lower molecular weight compared to the starting polysaccharide (220 kDa, polydispersity index 1.8), the tetrabutylammonium salt of HA (HA-TBA), and hyaluronic-((2-aminoethyl)-carbamate) acid-ethylenediamine (HA-EDA) were synthesized as previously described (Fiorica et al., 2013; Palumbo et al., 2012). 1-Ethyl-3-(3-dimethylaminopropyl)-carbodiimide (EDC), N-hydroxysuccinimide (NHS), (4-morpholineethanesulfonic acid (MES) buffer, Sephadex G25 resin, and heparin (2.5 kDa) were kindly provided by Laboratorio Derivati Organici (Milan, Italy). Alexa Fluor 488-Hydroxylamine, and customized panels for Luminex (ProcartaPlex) were obtained from Thermo Fisher Scientific (Waltham, MA, USA). Human umbilical vein endothelial cells (HUVECs, catalog number C0035C) and human dermal fibroblasts (catalog number C0135C) were purchased from Life Technologies (Carlsbad, CA, USA). Dulbecco's phosphate buffered saline (DPBS), bovine testicular hyaluronidase (HAse), Dulbecco's Modified Eagle Medium (DMEM), and fetal bovine serum (FBS) were all purchased from Sigma-Aldrich (St. Louis, MO, USA). Seventy-five-cm^2 tissue flasks were purchased from Costar Corning Inc. (Costar, NY, USA). Alpha-Minimum Essential Medium (MEM) was purchased from Gibco (Thermo Fisher Scientific). *In vitro* angiogenesis assay kit and Amicon Ultra-15 centrifugal filter units were purchased from Millipore (Billerica, MA, USA). Six-well plastic plates were purchased from Costar Corning Inc.

2.1. Synthesis and characterization of heparin-free and heparinized HA-EDA/HA sponges

Two hundred mg of freeze-dried HA-EDA and 20 mg of HA were mixed and dispersed in 4 ml of double-distilled water (DDW) at 40 °C for at least 24 h. Subsequently, EDC and NHS were added at a molar ratio of 0.25 between EDC/NHS and the pendant free amino groups of the HA-EDA/HA sponge, and the dispersion was incubated at 37 °C overnight. The resulting hydrogel was frozen at −80 °C, followed by freeze-drying to obtain a porous, sponge-like structure. The obtained material was then rehydrated, washed with DDW, and cut into cylindrical samples with a diameter and length of 1 cm, which were further freeze-dried.

The heparinization of HA-EDA/HA sponges was conducted as previously described (Pitarresi et al., 2014), with slight modifications. Briefly, heparin was dissolved in MES buffer (pH 5.5) at a concentration of 2 % w/v in the presence of an equimolar amount (relative to the heparin repetitive units) of EDC/NHS. After 2 h of incubations at 37 °C, an appropriate volume of the heparin solution was poured onto the pre-weighted, freeze dried HA-EDA/HA sponge to satisfy a theoretical molar ratio of heparin repetitive units/EDA groups equal to 1 (starting from 10 mg of HA-EDA, 300 μl of heparin solution was poured). Following 24 h incubation at 37 °C, the sponges were washed with DDW and subsequently freeze-dried. Scanning electron microscopy was performed on heparin-free (hep-) and heparinized (hep +) HA-EDA/HA sponges to record energy-dispersive X-ray (EDX) spectra using a PhenomX instrument (Alfatest srl, Milan, Italy). To investigate the morphology of freeze-dried sponges, samples were sputter coated using a Luxor^{Au} gold coater (Alfatest) and subjected to scanning electron microscope (SEM) analysis.

To determine the heparinization degree, HA-EDA/HA sponges were functionalized with fluorescently labeled heparin using Alexa Fluor 488-Hydroxylamine. The reaction was carried out in MES buffer at pH 5.5, with a heparin concentration of 2 % w/v. The carboxylic groups of the sulfated polysaccharide were activated using EDC/NHS, as previously described (Pitarresi et al., 2014). The molar ratio between EDC/NHS and the repetitive units of heparin was set at 0.005. An equimolar amount of Alexa Fluor 488-Hydroxylamine relative to EDC/NHS was added to the activated heparin solution, and the reaction was conducted for 24 h at 37 °C. The resulting product was purified using gel permeation chromatography with Sephadex G25 and DDW as the mobile phase, followed by freeze-drying. The heparinization degree was indirectly determined by assessing the quantity of unbound heparin recovered after washing the sponge.

Swelling experiments for both hep- and hep + HA-EDA/HA sponges were conducted in DPBS at pH 7.4 and 37 °C. Each sample was weighted and then immersed in DPBS for 48 h. Subsequently, the excess buffer was removed, and the sample was reweighted. The swelling ratio (q) was calculated as the ratio between the weight of the swollen hydrogel and the weight of the freeze-dried sponge.

Chemical hydrolysis over a 30-day period, was carried out on hep- and hep + HA-EDA/HA sponges. Specifically, dried sponges were initially weighted and then incubated at 37 °C in DPBS at pH 7.4. At specified time intervals, samples were washed with DDW, freeze-dried, and carefully weighted to recorder the loss of weight undertaken. The results were expressed as a percentage of the recovered weight relative to time.

Enzymatic hydrolysis was carried out on hep- and hep + HA-EDA/HA sponges over a 24-hour period, as previously described (Bitter & Muir, 1962; Palumbo et al., 2015). In brief, freeze-dried sponges were incubated at 37 °C in DPBS at pH 7.4, with or without bovine testicular hyaluronidase (10 U/ml). After 24 h, the quantity of released HA soluble fragments was quantified using the carbazole assay. The results were expressed as a percentage of released uronic acid over time, with the values obtained from the carbazole assay on the aqueous dispersion of HA-EDA, HA, and heparin (mixed at the appropriate weight ratio) considered as 100 %. To determine whether the presence of unfunctionalized HA could impact the hydrolytic and enzymatic stability of the

sponges, the carbazole assay was also performed on hep- and hep + HA-EDA crosslinked sponges, and the results were compared with the carbazole assay results of hep- and hep + HA-EDA/HA sponges.

2.2. Cell source

Fetal skin biopsies were obtained from 16- to 22-week gestation human fetuses from therapeutic abortions, following a protocol approved by IRCCS ISMETT's Institutional Research Review Board (IRRB/00/15) and the ethics committee. A signed informed consent was obtained from each donor. MSCs were isolated from fetal dermis using a non-enzymatic tissue outgrowth technique, as previously described (Chinnici et al., 2014).

2.3. Collection of secretome and quantification of growth factors and chemokines

Human fetal dermal MSCs were isolated and characterized as previously described (Chinnici et al., 2014). The cells were grown in DMEM with 10 % FBS until reaching 80 % confluence. Then, serum-free alpha-MEM was added to cultured cells, and secretome was collected 24 h later. The collected secretome was subjected to centrifugation at 2000 x g for 10 min to remove cell debris. The secreted proteins were quantified using Luminex xMAP technology (Luminex 200; Luminex Corp. Austin, TX, USA) along with a customized panel of growth factors and chemokines relevant to angiogenesis and wound healing, including vascular endothelial growth factor (VEGF)-A, hepatocyte growth factor (HGF), interleukin-6 (IL-6), interleukin-8 (IL-8), stromal derived factor (SDF)-1alpha, growth regulated oncogene (GRO)-alpha and monocyte chemoattractant protein (MCP-1). Briefly, both undiluted and 1:10 diluted secretome samples were loaded into the multiplex assay and processed in accordance with the manufacturer's instructions. The concentration of soluble factors was calculated using a software provided by the manufacturer and expressed in pg/ml. The results were subsequently normalized based on the number of adherent MSCs.

2.4. Functional testing of secretome in in vitro cell-based assays

The secretome capacity to induce the formation of vessel-like structures in HUVECs was assessed by an *in vitro* angiogenesis assay, as previously described (Gaetani et al., 2018). Briefly, 10,000 serum-starved HUVECs were suspended in normal culture medium (used as negative control) or secretome. These cells were then plated onto Matrigel-coated 96-wells and incubated in a humidified atmosphere with 5 % CO_2 at 37 °C. Capillary formation was continuously monitored under an inverted microscope (Olympus CKX41, Tokyo, Japan) equipped with a camera (Olympus U-TV0.5XC-3). Each pattern observed was assigned a score ranging from 0 to 5, according to manufacturer's specifications. Visual patterns were determined based on photographs, and three images were evaluated per sample.

The migratory response of human fibroblasts induced by secretome was evaluated using the xCELLigence Real-Time Cell Analyzer (RTCA) dual purpose (DP) instrument (Acea Biosciences Inc., San Diego, CA, USA), as previously described (Chinnici et al., 2020). In brief, serum-free culture medium (used as negative control) or secretome was added to each well of the lower chamber of the Cellular Invasion/Migration (CIM)-plate. Subsequently, 30,000 serum-starved fibroblasts were suspended in serum-free culture medium and placed in the upper chamber. The device was incubated at 37 °C in a humidified atmosphere containing 5 % CO_2, and the migration of fibroblasts was recorded every 15 min over a 7-hour period. The results were expressed as cell index (CI) and presented as the mean from duplicate wells, along with the standard deviation (SD), at a 7-hour time point. Data analysis was conducted using the RTCA Software 1.2 of the xCELLigence system.

2.5. In vitro release kinetics of secretome from HA-EDA/HA hydrogels

Secretome from different MSC samples was pooled and concentrated 5-fold by ultrafiltration using 3 kDa molecular weight cut-off filters (Amicon Ultra-15 centrifugal filter unit). Hep- and hep + sponges, each measuring 1 cm^2 in size with a thickness of 0.5 cm, were plated in triplicate onto 12-well plastic plates (Corning). Each sponge was rehydrated with 200 μl of concentrated secretome, and 600 μl of DPBS were added to the surrounding space of the plate. The resulting hydrogels were incubated at 37 °C in a humidified atmosphere with 5 % CO_2. Aliquots of released secretome were collected at predetermined time points (24 hrs, 48 hrs, and then every 3 days) for 30 days. To maintain consistent volumes, the collected secretome at each time point was immediately replaced by adding an equal volume of DPBS. The collected secretome aliquots were stored at −80 °C until Luminex quantification or *in vitro* cell-based assays. Cumulative release was calculated by summing the amounts of soluble factor released at each time point and comparing them to the initially loaded amount. The functional activity of the hydrogel-released secretome at each time point was assessed in tube formation assay and in cell migration assay, as described above.

2.6. Statistical analysis

For secretome collection, MSC samples from six different donors were used. Differences between two groups were assessed using a two-tailed unpaired Student's *t*-test, and statistical significance was set at $p \leq 0.05$. Cumulative release data from three independent experiments were analyzed using Origin and expressed as mean ± SD. Cell migration data from three independent experiments were analyzed using GraphPad Prism 6.0 and expressed as mean ± SD.

3. Results

3.1. Production and characterization of HA-EDA/HA sponges

The derivatization degree in EDA ($DD\%_{EDA}$) of HA resulted in 60 ± 5 mol%. Pendant EDA groups were exploited to allow a carbodiimide mediated crosslinking of the mixed dispersion HA-EDA/HA. The dispersion was finally freeze-dried to produce porous 3D sponge-like scaffolds, which were later dehydrated with secretome to yield hydrogels (Fig. 1A). The amount of activating EDC/NHS was determined to consume no more than 25 % of the EDA groups on the HA-EDA derivative, ensuring the availability of free EDA groups for heparin functionalization, which was accomplished through carbodimide chemistry directly on preformed sponges. EDX analysis confirmed the presence of a sulfur peak on the hep + sponge, suggesting successful heparin tethering (Fig. 1B). The amount of linked heparin was 190 μg ± 19 μg per mg of dried sponge confirming a good efficiency of the heparinization procedure since about 30 % of the starting amount of the polysaccharide is recovered in the sponge. In terms of physical characterization, the hep + hydrogel exhibited a slightly higher swelling ratio (q) compared to the hep- hydrogel (19.42 ± 1.03 vs 17.22 ± 0.93). Furthermore, chemical hydrolysis experiments revealed that the hep + hydrogels lost 60 % of their weight, while the hep- hydrogel lost 30 % of their weight, following extended hydrolysis (10 days) in DPBS (Fig. 1C). Both hep + and hep- hydrogels released a similar amount of uronic acid (approximately 10 %) during the first hour of incubation in DPBS (data not shown). Furthermore, the enzymatic hydrolysis performed with 24-hour incubation with 10 U/ml HAase, revealed that the hep + hydrogel released 22 % uronic acid compared to 10–15 % released by the hep- hydrogel (Table 1). No significant differences in terms of uronic acid release were observed between HA-EDA/HA and HA-EDA hydrogels, these latter used as control (Table 1). SEM analysis indicated a highly porous structure of the freeze-dried HA-EDA/HA sponge (Fig. 1D).

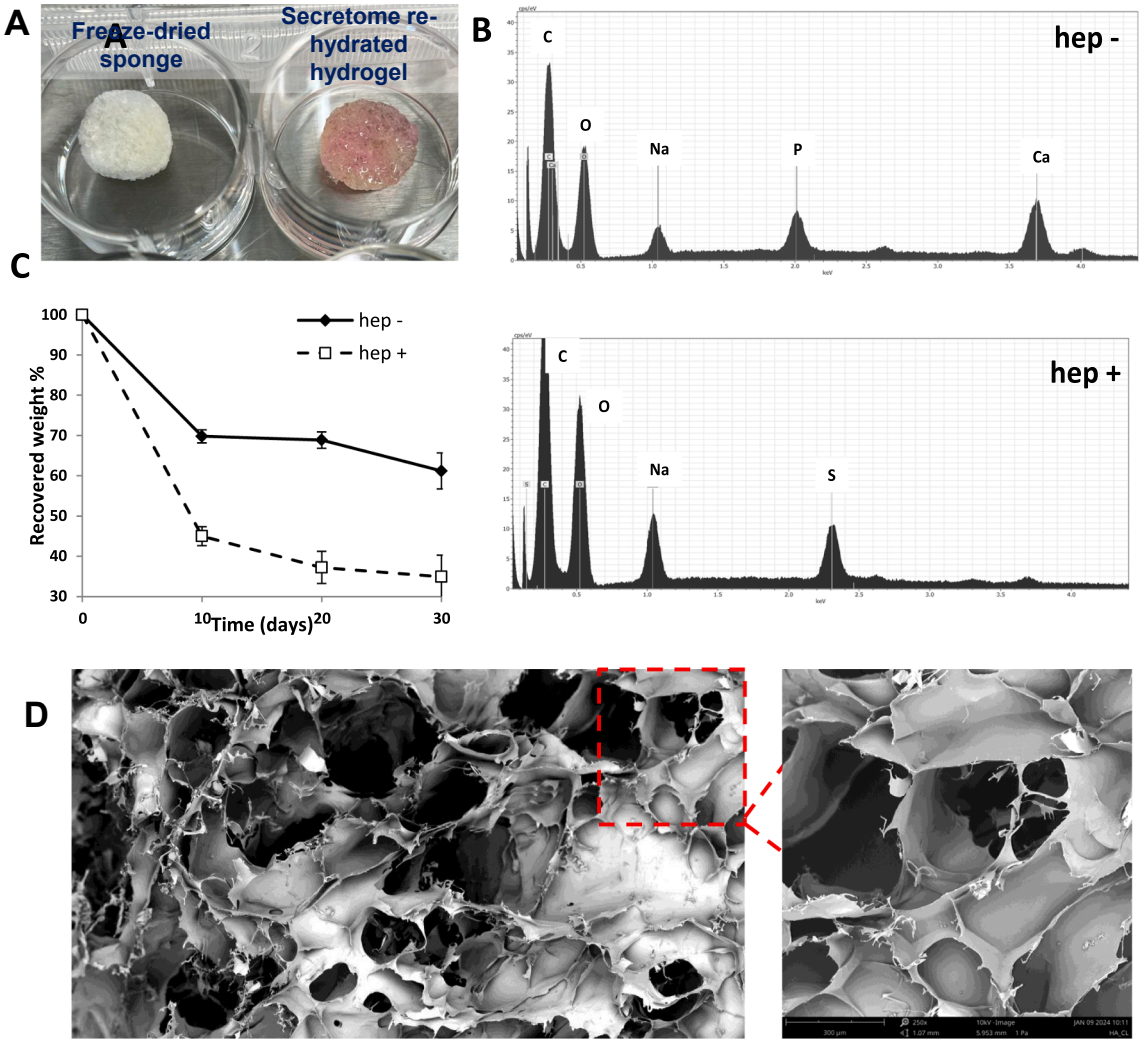

Fig. 1. Morphological analysis of sponges, including enzymatic and hydrolytic profile. (A) A freeze-dried HA-EDA/HA sponge before and after rehydration with secretome, resulting in the formation of a hydrogel. (B) EDX spectra analysis of hep- and hep + sponges showing the peaks related to the surface elements. (C) Chemical hydrolysis of hep- and hep + sponges incubated in DPBS at 37 °C for 30 days. The results were expressed as recovered weight as a percentage of the starting weight of sponges over time. (D) SEM analysis of HA-EDA/HA freeze-dried sponges. The larger image is obtained by mapping a surface area of 8.4 mm^2. EDX: energy-dispersive X-ray; hep: heparin.

Table 1
Enzymatic hydrolysis of the sponges. Amount of soluble HA fragments expressed as a percentage of uronic acid released from hep + and hep- sponges following incubation with DPBS or 10 U/ml of HAase for 24 h.

	Hep+HA-EDA/HA	Hep-HA-EDA/HA	Hep+HA-EDA	Hep-HA-EDA
DPBS pH 7.4	13.06 ± 3.2 %	13.97 ± 1.15 %	11.42 ± 5.0 %	10.34 ± 8.9 %
HAse 10 U/ml	22.50 ± 4.0 %	10.18 ± 1.9 %	22.3 ± 5.0 %	15.37 ± 2.6 %

Table 2
Concentration of growth factors and chemokines in the 5-fold concentrated secretome prior to loading into the sponges.

Soluble factors	pg/ml
VEGF	14767 ± 323
HGF	2008 ± 352
IL-6	2060 ± 581
IL-8	7298 ± 608
SDF-1 alpha	8157 ± 1681
GRO-alpha	1882 ± 33
MCP-1	5100 ± 639

The plotted values (mean ± SD) represent aliquots of secretome collected from six samples (n = 6).

3.2. In vitro release kinetics of secretome from hep- and hep + hydrogels

The amount of growth factors and chemokines in the 5-fold concentrated secretome is shown in Table 2. The release kinetics from the hep- hydrogel (red dotted line) demonstrated a gradual release of factors, with a peak occurring at day 18 for GRO-a, day 16 for MCP-1, day 12 for SDF-1 alpha IL-6 and IL-8, day 10 for HGF, and as earlier as day 6 for VEGF-A (Fig. 2A, B). Cumulative release indicated a 60–75 % release of IL-8, IL-6, SDF-1 alpha, GRO-alpha and HGF, a 100 % release of VEGF-A, whereas IL-6 was released up to 22 % (Fig. 2A, B).

The release kinetics of chemokines from the hep + hydrogel (black dotted line) were significantly different from those of the hep- hydrogel, indicating effective retention of these factors within the hydrogel (Fig. 2A). Conversely, the release kinetics of growth factors, particularly HGF, from the hep + hydrogel indicated lower retention. In fact, 50 % of VEGF-A was released within 6 days, whereas almost the entirety of HGF

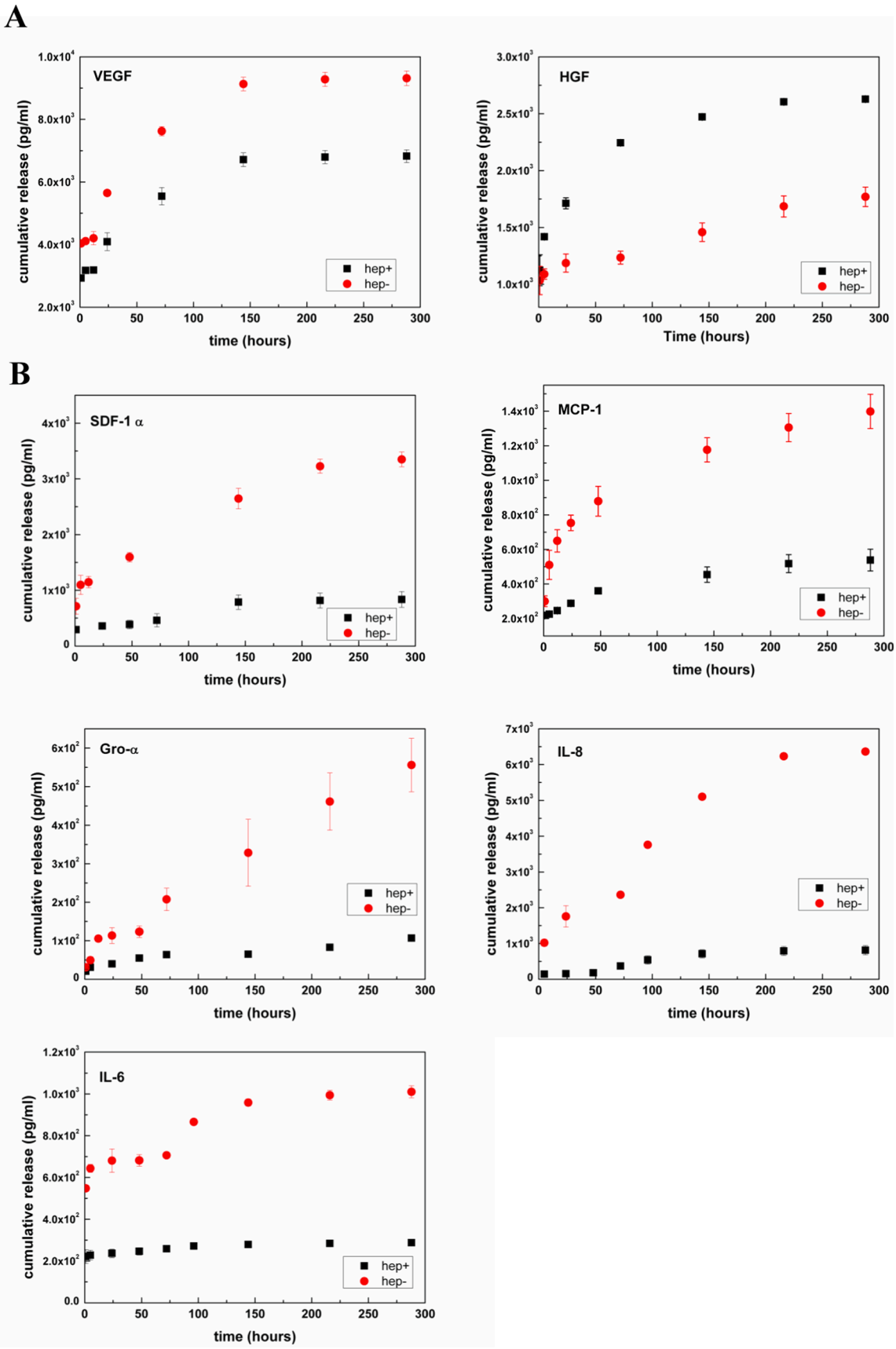

Fig. 2. Release kinetics of growth factors and chemokines from hep- (red dotted line) and hep+ (black dotted line) hydrogels, performed at 37 °C in a humidified atmosphere with 5 % CO_2 in DPBS. (A) Cumulative release of growth factors VEGF-A and HGF. (B) Cumulative released of chemokines SDF-1 alpha, GRO-alpha, MCP-1, IL-6 and IL-8. The concentrations of soluble factors at each time point were quantified using a customized Luminex panel and expressed as pg/ml over time (mean ± SD, n = 3). The factors concentrations were also plotted as cumulative release (Origin) and expressed as a percentage over time.

(approximately 90 %) was released within 12 days (Fig. 2B).

3.3. Functional testing of released secretome: In vitro assays of angiogenesis and cell migration

Positive control, HUVECs suspended in 5-fold concentrated secretome achieved the "close polygons" pattern (score 4) within six hours

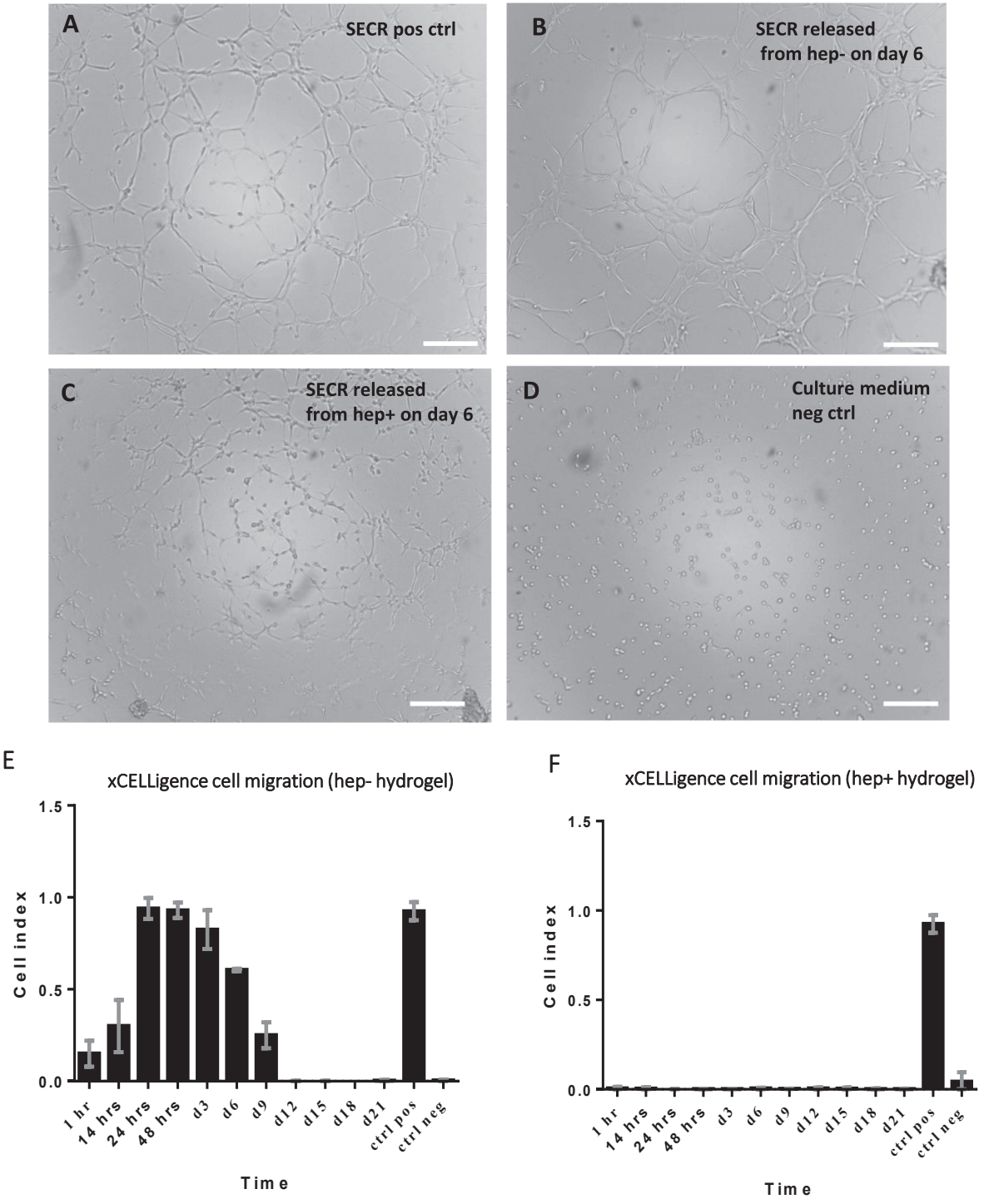

Fig. 3. Functional testing of secretome released from the HA-EDA hydrogel. *In vitro* angiogenesis assay. Representative images were captured 6 h after seeding HUVECs onto Matrigel. (A) Positive control: HUVECs in secretome before loading into the sponge. (B) HUVECs in secretome released from the hep- hydrogel at the day 6 time point. (C) HUVECs in secretome released from the hep + hydrogel at the day 6 time point. (D) Negative control: HUVECs in serum-free normal culture medium (alpha-MEM). *In vitro* real-time migration of fibroblasts recorded with XCELLigence for 7 h. Secretome before loading into the sponge and serum-free alpha-MEM were used as positive and negative control, respectively. (E) Fibroblasts migration induced by secretome released from the hep- hydrogel at different time points. (F) Fibroblasts migration induced by secretome released from the hep + hydrogel at different time points. Secr: secretome; pos ctrl: positive control; neg ctrl: negative control; hep: heparin. Scale bars: 200 μm.

(Fig. 3A). A similar pattern (score 4) was achieved by HUVECs suspended in secretome released from the hep- hydrogel at day 1 to day 12 time points (Fig. 3B representing day 6 release). A "sprout of new capillary tubes" pattern (score 3) was observed when HUVECs were suspended in secretome released from hep + hydrogel up to day 6 (Fig. 3C representing day 6 release The "individual cells, well separated" pattern (corresponding to score 0) was observed in the negative control, where HUVECs were suspended in serum-free culture medium (Fig. 3D), as well as in HUVECs suspended in secretome released at later time points (data not shown).

Secretome released from the hep- hydrogel from 1 h to day 6 induced a migratory response of fibroblasts, achieving CI values similar to those of the positive control, which represents cell migration induced by secretome before its loading into the hydrogel. A lower migratory response was observed at later time points (e.g., day 9 release), while even later time points indicated an absence of cell migration with CI values similar to those of negative controls (Fig. 3E). The CI values of secretome released from the hep + hydrogel indicated an absence of cell migration and values similar to those of negative controls at all the assessed time points (Fig. 3F).

4. Discussion

Several challenges must be addressed before secretome-based treatments can be translated into clinically relevant therapies. One crucial challenge concerns the delivery of soluble factors to the healing tissue, as it can significantly impact treatment efficacy. Therefore, it is necessary to develop delivery strategies that render secretome-based therapy more clinically applicable (Gwam et al., 2021). A limitation associated with the use of delivery devices based on physically crosslinked HA is the relatively short *in vivo* half-life of the biomaterial, which ranges from a few hours to 2–3 days, depending on the type of tissue being treated (Carruthers & Carruthers, 2007; Xu et al., 2012). Here, the HA derivative HA-EDA was synthesized using a well-established chemical crosslinking procedure (Palumbo et al., 2012b; Palumbo et al., 2015). Briefly, the hydroxyl groups of HA were functionalized with EDA, and unfunctionalized HA was incorporated to enhance water retention and the compactness of the biomaterial. This process resulted in the formation of a HA-EDA/HA with a 3D sponge-like structure following freeze-drying. Interestingly, the HA-EDA/EDA sponge acquired a hydrogel consistency upon rehydration with secretome.

Additionally, to enhance the affinity of the HA-based hydrogel for certain secretome molecules, the unreacted pendant EDA groups were functionalized with heparin, serving as a substitute for the natural ECM component heparan sulfate. The newly obtained heparinized hydrogel displayed a greater water affinity when compared to the hep- hydrogel, suggesting a potential enhancement in hydrophilicity attributed to the presence of heparin sulfate groups. Nonetheless, neither hydrogel type exhibited significant shape alterations during release kinetics analysis (one month at 37 °C), and both demonstrated partial degradation without complete breakdown (no significative fragmentation and retention of their cylindrical form). This observation was supported by a similar swelling ratio (q) for both hydrogel types.

Heparin crosslinking may also contribute in increasing the sensitivity of the hydrogel to enzymatic digestion. From an applicative perspective, the potential high sensitivity to both chemical and enzymatic hydrolysis could be harnessed to achieve a faster reabsorption of the hep + hydrogel when applied to the wound bed (Fronza et al., 2014). Conversely, a hydrogel with slower reabsorption rates, such as the hep- hydrogel, may be more suitable for applications where a complete degradation of the biomaterial is not necessary, such as topical treatments that involve removing hydrogel patches during repeated applications.

Both hep + and hep- hydrogels were capable of accommodating substantial amounts of soluble factors contained within 200 μl of concentrated secretome. As expected, the hep- hydrogel exhibited a greater capacity to sustain the release of soluble factors compared to the hep + hydrogel. Specifically, 60–75 % of the initially loaded amounts were released over an average period of 12 days. The only exception was the low release rates of IL-6 (22 %), possibly attributed to non-specific adsorption on the biomaterial.

The observed low release rates of chemokines (4–15 % over a period of 8–9 days) in the hep + hydrogel suggest a successful role of heparin crosslinking in enhancing the affinity of the HA hydrogel for these molecules. Nonetheless, despite the well-documented high affinity of growth factors for heparin (Zhao et al., 2012; Zhou et al., 1999), VEGF-A and HGF exhibited significantly higher release rates (50 % and 90 % within 6 and 12 days, respectively) from hep + hydrogel compared to chemokines. This discrepancy may be attributed to a combination of concentration and molecular weight of these molecules, influencing their diffusion through the porous structure of the hydrogel and leading to competition for heparin binding sites. Accordingly, the larger molecular weight (34 kDa) and lower concentration (approximately 2000 pg/ml) of HFG, in contrast to the smaller chemokines and the highly concentrated (approximately 14000 pg/ml) VEGF-A, may explain its rapid release from the hep + hydrogel. The affinity for heparin (K_D values) and molecular weights of the considered molecules are detailed in Table 3. Interestingly, aliquots of secretome released from the hep- hydrogel, but not from the hep + hydrogel, over a 6–9-day period, elicited biological responses in target cells with efficiencies comparable to those of the positive controls. This observation suggests that the concentration of released factors was sufficient to support the desired cell responses.

Overall, the combination of the HA-EDA/HA sponge with MSC secretome to form a hydrogel seems well-suited for topical applications of regenerative medicine. The sustained release of secretome from the hep- hydrogel may be indicated for treatments with extended durations, particularly those necessitating repeated applications to a wound. Conversely, the hep + hydrogel can serve as a depot enriched with key molecules that facilitate the wound healing process. Indeed, the retention of chemokines from the hep + hydrogel at the wound bed has the potential to promote the recruitment of resident cells and effectively elicit the endogenous repair process. Moreover, given its high sensitivity to enzymatic digestion, the hep + hydrogel could be further tailored to achieve controlled release of secretome molecules. In this context, the hep + hydrogel could be targeted by various *in vivo* enzymes, such as heparanase, whose activity increases during wound healing (Gurtner et al., 2008).

5. Conclusions

The conventional single-factor approach for wound healing applications has frequently fallen short of meeting expectations in numerous clinical trials (Beohar et al., 2010; Robson, 2003). In contrast, secretome-based therapy, which involves a combination of bioactive molecules, offers more promising prospects for success. Our HA-based hydrogel integrated with secretome shows potential for addressing chronic skin wounds. This versatile device can function as a topical

Table 3
Affinity for heparin (K_D) and molecular weights of the considered secretome factors.

Soluble factors	K_D	MW
VEGF-A	10^{-8} M	27 kDa
HGF	10^{-9} M	34 kDa
SDF-1 alpha (CXCL-12)	10^{-8} M	8 kDa
MCP-1 (CCL-2)	NA	13 kDa
GRO-alpha (CXCL-1)	NA	11 kDa
IL-6	10^{-7} M	11 kDa
IL-8	10^{-7} M	22 kDa

K_D values were obtained from the heparin-protein interaction dataset. NA: not available. MW: molecular weight.

depot sustaining the release of bioactive molecules facilitating wound repair. Furthermore, the presence of heparin underscores the significance of tailoring the device to achieve the desired release schedule. While the integration of MSCs with biomaterials to form engineered tissues (Li et al., 2018; Wagenbrenner et al., 2021) or for cell delivery (Snyder et al., 2014) is a well-documented approach, the direct incorporation of secretome into a biomaterial sustaining or controlling its release is described in only a limited number of studies (Brennan et al., 2020; Liu et al., 2019; Shoma Suresh et al., 2020). *In vivo* animal models of disease are essential for elucidating the safety and efficacy of this approach, facilitating the translation of these findings into clinically relevant results.

CRediT authorship contribution statement

Fabio Salvatore Palumbo: Conceptualization, Methodology, Data curation, Writing. **Calogero Fiorica:** Conceptualization, Methodology, Writing. **Anna Paola Carreca:** Methodology. **Gioacchin Iannolo:** Conceptualization, Methodology. **Giovanna Pitarresi:** Conceptualization, Methodology. **Giandomenico Amico:** Methodology, Data curation. **Gaetano Giammona:** Conceptualization, Resources. **Pier Giulio Conaldi:** Conceptualization, Funding acquisition. **Cinzia Maria Chinnici:** Conceptualization, Methodology, Data curation, Writing – original draft, Writing – review & editing.

Declaration of competing interest

The authors declare that they have no known competing financial interests or personal relationships that could have appeared to influence the work reported in this paper.

Data availability

No data was used for the research described in the article.

Acknowledgements

The authors wish to thank the Gynecology Unit (Ospedale Civico, Palermo) for providing the human fetal skin biopsies. This work was supported by the Italian Ministry of Education, University and Research (NOP for Research and Competitiveness 2007–2013, IRMI (CTN01_00177_888744).

References

Beohar, N., Rapp, J., Pandya, S., Losordo, D.W., 2010. Rebuilding the damaged heart: the potential of cytokines and growth factors in the treatment of ischemic heart disease. J. Am. Coll. Cardiol. 56 (16), 1287–1297. https://doi.org/10.1016/J.JACC.2010.05.039.

Bitter, T., Muir, H.M., 1962. A modified uronic acid carbazole reaction. Anal. Biochem. 4 (4), 330–334. https://doi.org/10.1016/0003-2697(62)90095-7.

Brennan, M., Layrolle, P., Mooney, D.J., 2020. Biomaterials functionalized with MSC secreted extracellular vesicles and soluble factors for tissue regeneration. Adv. Funct. Mater. 30 (37) https://doi.org/10.1002/ADFM.201909125.

Caplan, A.I., 2017. Mesenchymal Stem Cells: Time to Change the Name! Stem Cells Transl. Med. 6 (6), 1445–1451. https://doi.org/10.1002/SCTM.17-0051.

Carruthers, A., Carruthers, J., 2007. Non-animal-based hyaluronic acid fillers: scientific and technical considerations. Plast. Reconstr. Surg. 120 (6 Suppl) https://doi.org/10.1097/01.PRS.0000248808.75700.5F.

Censi, R., Di Martino, P., Vermonden, T., Hennink, W.E., 2012. Hydrogels for protein delivery in tissue engineering. J. Control. Release 161 (2), 680–692. https://doi.org/10.1016/J.JCONREL.2012.03.002.

Chai, Q., Jiao, Y., Yu, X., 2017. Hydrogels for Biomedical Applications: Their Characteristics and the Mechanisms behind Them 3. https://doi.org/10.3390/GELS3010006.

Chinnici, C.M., Amico, G., Monti, M., Motta, S., Casalone, R., Li Petri, S., Spada, M., Gridelli, B., Conaldi, P.G., 2014. Isolation and characterization of multipotent cells from human fetal dermis. Cell Transplant. 23 (10), 1169–1185. https://doi.org/10.3727/096368913X668618.

Chinnici, C.M., Amico, G., Gallo, A., Iannolo, G., Cuscino, N., Vella, S., Carcione, C., Nascari, D., Conaldi, P.G., 2020. Small Extracellular Vesicles from Human Fetal Dermal Cells and Their MicroRNA Cargo: KEGG Signaling Pathways Associated with Angiogenesis and Wound Healing. Stem Cells Int. 2020 https://doi.org/10.1155/2020/8889379.

Drago, D., Cossetti, C., Iraci, N., Gaude, E., Musco, G., Bachi, A., Pluchino, S., 2013. The stem cell secretome and its role in brain repair. Biochimie 95 (12), 2271–2285. https://doi.org/10.1016/J.BIOCHI.2013.06.020.

Fiorica, C., Pitarresi, G., Palumbo, F.S., Di Stefano, M., Calascibetta, F., Giammona, G., 2013. A new hyaluronic acid pH sensitive derivative obtained by ATRP for potential oral administration of proteins. Int. J. Pharm. 457 (1) https://doi.org/10.1016/j.ijpharm.2013.09.005.

Freudenberg, U., Zieris, A., Chwalek, K., Tsurkan, M.V., Maitz, M.F., Atallah, P., Levental, K.R., Eming, S.A., Werner, C., 2015. Heparin desulfation modulates VEGF release and angiogenesis in diabetic wounds. J. Control. Release 220 (Pt A), 79–88. https://doi.org/10.1016/J.JCONREL.2015.10.028.

Gaetani, M., Chinnici, C.M., Carreca, A.P., Di Pasquale, C., Amico, G., Conaldi, P.G., 2018. Unbiased and quantitative proteomics reveals highly increased angiogenesis induction by the secretome of mesenchymal stromal cells isolated from fetal rather than adult skin. J. Tissue Eng. Regen. Med. 12 (2), e949–e961. https://doi.org/10.1002/TERM.2417.

Gillitzer, R., Goebeler, M., 2001. Chemokines in cutaneous wound healing. J. Leukoc. Biol. 69 (4), 513–521. https://doi.org/10.1189/JLB.69.4.513.

Giovannelli, L., Bari, E., Jommi, C., Tartara, F., Armocida, D., Garbossa, D., Cofano, F., Torre, M.L., Segale, L., 2023. Mesenchymal stem cell secretome and extracellular vesicles for neurodegenerative diseases: Risk-benefit profile and next steps for the market access. Bioact. Mater. 29, 16–35. https://doi.org/10.1016/J.BIOACTMAT.2023.06.013.

Gurtner, G. C., Werner, S., Barrandon, Y., & Longaker, M. T. (2008). Wound repair and regeneration. *Nature 2008 453:7193*, *453*(7193), 314–321. https://doi.org/10.1038/nature07039.

Gwam, C., Mohammed, N., Ma, X., 2021. Stem cell secretome, regeneration, and clinical translation: a narrative review. Annals of Translational Medicine 9 (1), 70. https://doi.org/10.21037/ATM-20-5030.

Huang, L., Wang, Y., Liu, H., Huang, J., 2017. Local injection of high-molecular hyaluronan promotes wound healing in old rats by increasing angiogenesis. Oncotarget 9 (9), 8241–8252. https://doi.org/10.18632/ONCOTARGET.23246.

Jiao, Y., Pang, X., Zhai, G., 2016. Advances in Hyaluronic Acid-Based Drug Delivery Systems. CurrentDrug Targets 17 (6), 720–730. https://doi.org/10.2174/1389450116666150531155200.

Li, L., Duan, X., Fan, Z., Chen, L., Xing, F., Xu, Z., Chen, Q., Xiang, Z., 2018. Mesenchymal Stem Cells in Combination with Hyaluronic Acid for Articular Cartilage Defects. Sci. Rep. 8 (1) https://doi.org/10.1038/S41598-018-27737-Y.

Liang, Y., He, J., Guo, B., 2021. Functional Hydrogels as Wound Dressing to Enhance Wound Healing. ACS Nano 15 (8), 12687–12722. https://doi.org/10.1021/ACSNANO.1C04206.

Liao, X., Yang, X., Deng, H., Hao, Y., Mao, L., Zhang, R., Liao, W., Yuan, M., 2020. Injectable Hydrogel-Based Nanocomposites for Cardiovascular Diseases. Front. Bioeng. Biotechnol. 8 https://doi.org/10.3389/FBIOE.2020.00251.

Liechty, W.B., Peppas, N.A., 2012. Expert opinion: Responsive polymer nanoparticles in cancer therapy. Eur. J. Pharm. Biopharm. 80 (2), 241–246. https://doi.org/10.1016/j.ejpb.2011.08.004.

Liu, F., Hu, S., Yang, H., Li, Z., Huang, K., Su, T., Wang, S., Cheng, K., 2019. Hyaluronic Acid Hydrogel Integrated with Mesenchymal Stem Cell-Secretome to Treat Endometrial Injury in a Rat Model of Asherman's Syndrome. Adv. Healthc. Mater. 8 (14) https://doi.org/10.1002/ADHM.201900411.

Miller, T., Goude, M.C., Mcdevitt, T.C., Temenoff, J.S., 2014. Molecular engineering of glycosaminoglycan chemistry for biomolecule delivery. Acta Biomater. 10 (4), 1705–1719. https://doi.org/10.1016/J.ACTBIO.2013.09.039.

Palumbo, F.S., Pitarresi, G., Fiorica, C., Matricardi, P., Albanese, A., Giammona, G., 2012. In situ forming hydrogels of new amino hyaluronic acid/benzoyl-cysteine derivatives as potential scaffolds for cartilage regeneration. Soft Matter 8 (18), 4918–4927. https://doi.org/10.1039/C2SM07310B.

Palumbo, F.S., Fiorica, C., Di Stefano, M., Pitarresi, G., Gulino, A., Agnello, S., Giammona, G., 2015a. In situ forming hydrogels of hyaluronic acid and inulin derivatives for cartilage regeneration. Carbohydr. Polym. 122, 408–416. https://doi.org/10.1016/J.CARBPOL.2014.11.002.

Palumbo, F.S., Fiorica, C., Pitarresi, G., Agnello, S., Giammona, G., 2015b. Interpenetrated 3D porous scaffolds of silk fibroin with an amino and octadecyl functionalized hyaluronic acid. *RSC*. Advances 5 (75). https://doi.org/10.1039/c5ra09400c.

Pitarresi, G., Fiorica, C., Palumbo, F.S., Rigogliuso, S., Ghersi, G., Giammona, G., 2014. Heparin functionalized polyaspartamide/polyester scaffold for potential blood vessel regeneration. Journal of Biomedical Materials Research - Part A 102 (5). https://doi.org/10.1002/jbm.a.34818.

Robson, M.C., 2003. Cytokine manipulation of the wound. Clin. Plast. Surg. 30 (1), 57–65. https://doi.org/10.1016/S0094-1298(02)00073-1.

Shoma Suresh, K., Bhat, S., Guru, B.R., Muttigi, M.S., Seetharam, R.N., 2020. A nanocomposite hydrogel delivery system for mesenchymal stromal cell secretome. Stem Cell Res Ther 11 (1). https://doi.org/10.1186/S13287-020-01712-9.

Snyder, T.N., Madhavan, K., Intrator, M., Dregalla, R.C., Park, D., 2014. A fibrin/hyaluronic acid hydrogel for the delivery of mesenchymal stem cells and potential for articular cartilage repair. J. Biol. Eng. 8 (1) https://doi.org/10.1186/1754-1611-8-10.

Tran, C., Damaser, M.S., 2015. Stem cells as drug delivery methods: application of stem cell secretome for regeneration. Adv. Drug Deliv. Rev. 82–83, 1–11. https://doi.org/10.1016/J.ADDR.2014.10.007.

Tsurkan, M.V., Hauser, P.V., Zieris, A., Carvalhosa, R., Bussolati, B., Freudenberg, U., Camussi, G., Werner, C., 2013. Growth factor delivery from hydrogel particle

aggregates to promote tubular regeneration after acute kidney injury. J. Control. Release 167 (3), 248–255. https://doi.org/10.1016/J.JCONREL.2013.01.030.
Vizoso, F.J., Eiro, N., Cid, S., Schneider, J., Perez-Fernandez, R., 2017. Mesenchymal Stem Cell Secretome: Toward Cell-Free Therapeutic Strategies in Regenerative Medicine. Int. J. Mol. Sci. 18 (9) https://doi.org/10.3390/IJMS18091852.
Wagenbrenner, M., Mayer-Wagner, S., Rudert, M., Holzapfel, B.M., Weissenberger, M., 2021. Combinations of Hydrogels and Mesenchymal Stromal Cells (MSCs) for Cartilage Tissue Engineering-A Review of the Literature. Gels (Basel. Switzerland) 7 (4). https://doi.org/10.3390/GELS7040217.
Xu, X., Jha, A.K., Harrington, D.A., Farach-Carson, M.C., Jia, X., 2012. Hyaluronic Acid-Based Hydrogels: from a Natural Polysaccharide to Complex Networks. Soft Matter 8 (12), 3280–3294. https://doi.org/10.1039/C2SM06463D.
Zhao, W., McCallum, S.A., Xiao, Z., Zhang, F., Linhardt, R.J., 2012. Binding affinities of vascular endothelial growth factor (VEGF) for heparin-derived oligosaccharides. Biosci. Rep. 32 (1), 71–81. https://doi.org/10.1042/BSR20110077.
Zhou, H., Casas-Finet, J.R., Coats, R.H., Kaufman, J.D., Stahl, S.J., Wingfield, P.T., Rubin, J.S., Bottaro, D.P., Byrd, R.A., 1999. Identification and dynamics of a heparin-binding site in hepatocyte growth factor. Biochemistry 38 (45), 14793–14802. https://doi.org/10.1021/BI9908641/SUPPL_FILE/BI9908641_S.PDF.